

The lattice contribution to the specific heat in tetramethylammonium tetrachlorometallates

This article has been downloaded from IOPscience. Please scroll down to see the full text article.

1990 J. Phys.: Condens. Matter 2 513

(<http://iopscience.iop.org/0953-8984/2/3/002>)

View [the table of contents for this issue](#), or go to the [journal homepage](#) for more

Download details:

IP Address: 171.66.16.96

The article was downloaded on 10/05/2010 at 21:28

Please note that [terms and conditions apply](#).

The lattice contribution to the specific heat in tetramethylammonium tetrachlorometallates

A López-Echarri, I Ruíz-Larrea and M J Tello

Departamento de Física de Materia Condensada, Facultad de Ciencias, Universidad del País Vasco, Apartado 644, Bilbao 48080, Spain

Received 6 June 1989, in final form 28 September 1989

Abstract. The lattice specific heat in tetramethylammonium tetrachlorometallates was calculated from accurate C_p measurements as well as from the available spectroscopic data. The experimental information on various members of this family and some related compounds was also used to analyse the various contributions to the lattice specific heat. The anharmonic correction was performed using the Nernst–Lindemann law, together with the elastic constants and with the thermal expansion coefficients. The frequencies of the Raman and infrared inactive modes were estimated from the active associated motions in related organic molecules. Einstein and Debye functions were used to calculate the harmonic specific heat from the phonon spectrum. The final result shows an excellent fit to the experimental data and provides a useful method to obtain a baseline for the calculation of the phase transition thermodynamic functions. This method has permitted us to study the specific heat contribution of the tetramethylammonium groups, which is also compared with the values obtained by other procedures. Finally, the main sources of errors are discussed.

1. Introduction

As is well known, incommensurate, ferroelectric and ferroelastic phases in tetramethylammonium tetrachlorometallates, $[\text{N}(\text{CH}_3)_4]_2\text{MCl}_4$ have been widely studied in the past ten years. Some recent reviews account for the general physical properties of these crystals under different experimental conditions (Gesi 1986). The characterisation of the various phases by structural (Wiesner *et al* 1967, Tanisaki and Mashiyama 1980, Hasebe *et al* 1982), dielectric (Sawada *et al* 1978a, b, Zangar *et al* 1983) and calorimetric measurements (Ruiz-Larrea *et al* 1981, 1988, Gómez-Cuevas *et al* 1981, 1983, Zubillaga *et al* 1988) as well as the influence of the hydrostatic pressure (Shimizu *et al* 1979, 1980), have allowed us to build up a common pressure–temperature phase diagram. Only the copper compound shows a somewhat anomalous behaviour, probably related to the high distortion of the inorganic tetrahedron due to the Jahn–Teller effect.

Within this framework, the thermodynamic properties of the phase transition sequences undergone by these crystals are of special interest in checking the validity of the models proposed for these phase sequences, the critical laws around the normal–incommensurate phase transitions and also to characterise the molecular disorder when temperature increases. For this purpose, specific heat measurements have been carried out in the past on these compounds (Ruiz-Larrea *et al* 1981, 1988, Gómez-Cuevas *et al*

1981, 1983, Zubillaga *et al* 1988) throughout the temperature range covering the phase sequence (60–330 K).

As far as we are aware, the spectroscopic data have never been used to estimate the lattice specific heat in these crystals. They have mainly been devoted to the study of the incommensurate behaviour and, in some cases, to the phase transition microscopic mechanisms. However, available Raman and infrared spectra (Takashige and Nakamura 1980, Srinivasan *et al* 1983, Tang *et al* 1986, Meekees 1987) which cover a wide frequency range could be useful for calculating the lattice contribution. This is a necessary task if we are interested in reliable information on the phase transition thermodynamic functions. These magnitudes are usually affected by noticeable errors, as they depend on the baseline used to approximate the lattice specific heat. Up to now, Debye functions with a temperature dependent Θ_D have been used as a provisional baseline (Ruiz-Larrea *et al* 1988, Zubillaga *et al* 1988). For this purpose, Θ_D versus temperature was extrapolated from its behaviour at both sides of the specific heat anomaly. However, this empirical fit is quite unsatisfactory not only due to the simplicity of the Debye model but also because we have omitted the anharmonic correction since elastic and expansivity measurements are frequently incomplete or are not available at all. These sources of errors cannot be disregarded in the case of $[\text{N}(\text{CH}_3)_4]_2\text{MCl}_4$ crystals, as they usually show a specific heat anomaly in a wide temperature range (typically 200–300 K), associated with a second-order normal–incommensurate phase transition.

With the exception of the copper crystal, the specific heats at constant pressure of $[\text{N}(\text{CH}_3)_4]_2\text{MCl}_4$ ($\text{M} = \text{Zn}, \text{Co}, \text{Mn}, \text{Fe}$) are practically coincident, once we exclude the phase transition anomalies. They attain a similar value ($\approx 52R$) in the common orthorhombic phase at room temperature. This result shows highly activated motions of the methyl groups (Ruiz-Larrea *et al* 1981) which have also been confirmed by NMR data (Blinic *et al* 1979, Sundaram *et al* 1986, Arumugam *et al* 1987). Below room temperature, the small discrepancies among the four specific heat curves can be assigned to differences of the respective anharmonic contributions and to small shifts of the frequency spectra. These divergences attain maximum values below 100 K (5% at 60 K). In this range the contribution of the high frequency modes as well as the anharmonic correction are very small and only the low frequency external modes of the organic and inorganic groups are expected to be shifted, as a natural consequence of the cation substitution.

The reasons mentioned above have permitted us to choose the $[\text{N}(\text{CH}_3)_4]_2\text{ZnCl}_4$ specific heat as representative of the remaining compounds, in order to calculate the lattice contribution. $[\text{N}(\text{CH}_3)_4]_2\text{ZnCl}_4$ is the most extensively studied among them and the elastic constants and the thermal expansion at room temperature are also known (Berger and Benoit 1984, Sawada *et al* 1985). This fact allows for a direct determination of the harmonic specific heat by means of the Nernst–Lindemann law. Inactive internal modes are also estimated by comparison with associated similar motions in related molecules in which those modes are active. Finally, a detailed analysis of the various contributions to the lattice specific heat is presented.

2. Anharmonic corrections

The general thermodynamic relation between the specific heat at constant stress (C_σ) and at constant strain (C_ϵ) (Gopal 1966)

$$C_\sigma - C_\epsilon = TVc_{ijkl}\alpha_{ij}\alpha_{kl} \quad (1)$$

(where \mathbf{c} and $\boldsymbol{\alpha}$ stand for the elastic constant and the thermal expansion tensors respect-

ively, T is the absolute temperature and V the molar volume), has been used to calculate C_v from the experimental data (C_p). In the following, C_v and C_p are respectively identified with C_ϵ and C_σ —once the difference between constant volume and constant geometry is discarded. As all the compounds studied show an orthorhombic phase with space group $Pmna$ above room temperature, the number of independent elastic constants is reduced to nine, whereas the independent thermal expansion coefficients are α_1 , α_2 and α_3 . Using the experimental values for these magnitudes at room temperature (Berger and Benoit 1984, Sawada *et al* 1985) and the calculated density: $\rho = 1.387 \text{ g cm}^{-3}$, we have obtained

$$C_p - C_v = 3.65R$$

which represents a noticeable correction (7%) for the experimental C_p . We should notice that similar calculations in the related inorganic compounds such as Rb_2ZnCl_4 or K_2SeO_4 lead to smaller differences between these magnitudes. As we shall see later, this result could be related to the elastic and expansivity properties of the tetramethylammonium groups due to the higher strength of their internal bonds.

Up to now, the temperature dependence of the elastic constants has not been fully determined. For this reason, the Nernst–Lindemann law

$$C_p - C_v = (V\alpha/k_T C_p^2) C_p^2 T = a C_p^2 T \quad (2)$$

(where V is the molar volume, $\alpha = V^{-1}(\partial V/\partial T)$ is the isobaric expansivity and $k_T = -V^{-1}(\partial V/\partial P)_T$ is the isothermal compressibility), has been used to determine the specific heat at constant volume in the temperature range 50–330 K. The coefficient $a = (V\alpha/k_T C_p^2)$ is considered to be constant for most solid substances (Gopal 1966) and can be evaluated at room temperature from the available experimental data. Figure 1 shows the C_p and C_v values for $[\text{N}(\text{CH}_3)_4]_2\text{ZnCl}_4$ with $a = 4.5 \times 10^{-6} \text{ R}^{-1} \text{ K}^{-1}$.

3. Normal modes in $[\text{N}(\text{CH}_3)_4]_2\text{ZnCl}_4$

3.1. Group theory

The room temperature structure of $[\text{N}(\text{CH}_3)_4]_2\text{ZnCl}_4$ (Wiesner *et al* 1967) shows only small distortions of the inorganic $[\text{ZnCl}_4]$ and the two organic $[\text{N}(\text{CH}_3)_4]$ tetrahedra. Group theory applied to the tetrahedral point group (T_d) shows the decomposition of the $3N - 6$ vibrational representation of the inorganic tetrahedron ($N = 5$), as a sum of the following irreducible representations:

$$\Gamma_9 = A_1 \oplus E \oplus 2T_2.$$

All of them are Raman active and only the modes T_2 are infrared active. The Zn–Cl bending modes are identified as E and T_2 , whereas the stretching modes are A_1 and T_2 . If we include the four methyl groups in the organic tetrahedron, a similar analysis shows that the $3N - 6$ vibrational representation for $N = 17$ decomposes as follows:

$$\Gamma_{45} = 3A_1 \oplus 4E \oplus 4T_1 \oplus 7T_2 \oplus A_2.$$

As happens with the modes of the inorganic tetrahedron, E and T_2 representations include the C–N bending modes, whereas the C–N stretching modes have A_1 and T_2 symmetries.

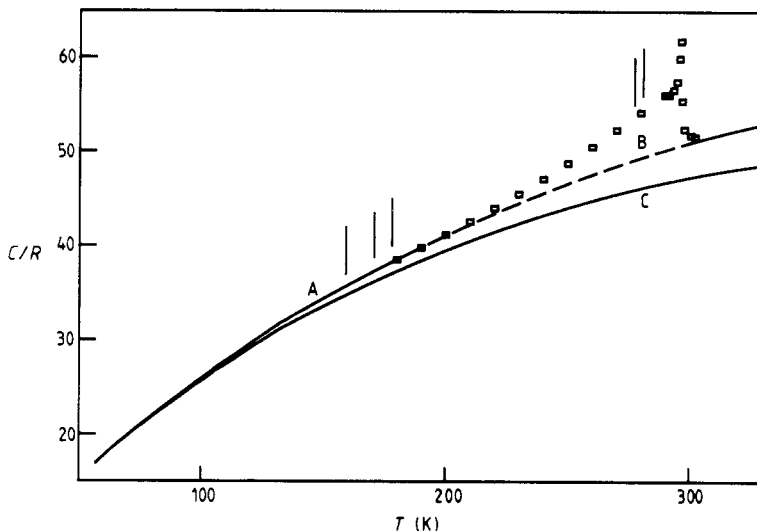


Figure 1. Anharmonic correction for the specific heat of $[\text{N}(\text{CH}_3)_4]_2\text{ZnCl}_4$. Only some experimental points (\square) have been plotted in the temperature range 180–300 K. Vertical lines show the positions of the various first-order phase transitions (Ruiz-Larrea *et al* 1981). Curve A has been fitted to the remaining experimental points by a least squares method. The broken curve B is a baseline obtained using a Debye function with temperature dependent Θ_D (see text). Curve C represents the specific heat at constant volume obtained by subtraction of the anharmonic contribution. This correction has been obtained from the elastic and thermal expansion data at room temperature and with the help of the Nernst–Lindemann law.

3.2. Frequency assignments

The available Raman spectra of $[\text{N}(\text{CH}_3)_4]_2\text{ZnCl}_4$ (Takashige and Nakamura 1980, Srinivasan *et al* 1983, Tang *et al* 1986, Meekees 1987, Meekees *et al* 1988) and of Rb_2ZnCl_4 (Petzelt *et al* 1982, Echegut *et al* 1984), have permitted the assignment of the correct frequency values to all the active modes present in the $[\text{N}(\text{CH}_3)_4]_2\text{ZnCl}_4$ molecule. We should note the good correlation found between the ZnCl_4 internal frequencies in both compounds, which shows the independence of such modes on the surrounding crystal field.

The frequencies of the thirteen inactive internal modes with symmetries $T_2(4)$ and $A_2(1)$ have been estimated by the following methods. First of all, the three inactive modes T_1 associated with the C–H stretching are supposed to lie in the same frequency range as the remaining active modes for this vibrational state. These high frequency modes (around 3000 cm^{-1}) lead to a negligible contribution to the lattice specific heat ($<0.01\%$) and have been discarded in our calculations.

As we have no direct experimental information on the frequencies to be assigned to the remaining inactive modes, we have directed our attention to the vibrational states of some related methyl compounds such as the paraffins. In the case of ethane, two active C–H bending modes with symmetries A_{1g} and E_u of the point group D_{3d} correspond to two inactive T_1 modes of the tetrahedral point group T_d . The frequencies of these modes, 1420 cm^{-1} and 910 cm^{-1} , lie, as expected, in the range of the C–H bending modes of the tetramethylammonium group. Although small frequency shifts will arise from the

different hydrogen interaction in the compared molecules, the induced error in the specific heat calculation is expected to be negligible.

The specific heat obtained by Einstein functions associated with the identified frequencies shows an approximate deficit of $8R$ at room temperature if compared with the experimental values, even if we consider a saturated value for the rotational and translational degrees of freedom of the organic and inorganic groups. This observation suggests that low frequencies ($<300\text{ cm}^{-1}$) must be assigned to the remaining four inactive modes with symmetries $A_2(1)$ and $T_1(3)$. The former one corresponds to the Raman active mode A_{1u} of ethane. This mode describes the undeformed rotation of both methyl groups around the C–C axis with a frequency of 277 cm^{-1} (Warshel and Lifson 1970). In the case of the tetramethylammonium tetrahedron, our analysis shows that the invariant operations for the pseudovectors associated with the undeformed rotations of the four CH_3 groups around the C–N axes assign the uni-dimensional A_2 representation to the in-phase rotation of the methyl groups, whereas the tri-dimensional T_1 representation is related to the three allowed out-of-phase rotations.

As a confirmation of these suggestions, an empirical assignment of a 260 cm^{-1} common mean frequency to these four inactive modes leads to the best fit of the experimental specific heat curve. This assignment is in good agreement with the inelastic neutron scattering results on $[\text{N}(\text{CH}_3)_4]$ cations (Brun *et al* 1987). Although the low frequencies of these A_2 and T_1 modes could be highly dependent on the group environment, our estimation seems to be compatible with such results.

We will finally refer to the rotational and translational movements of the three basic tetrahedra in the $[\text{N}(\text{CH}_3)_4]_2\text{ZnCl}_4$ molecule, which account for the remaining 18 degrees of freedom. The difference between the experimental specific heat data at room temperature and the one arising from all the internal modes shows a value of $17R$, which can only be understood if a near saturated value is attained by the specific heat contribution of the external modes in the orthorhombic phase. As a consequence, the associated frequencies must be located in the low range of the vibrational spectrum, mostly below 100 cm^{-1} . This result also agrees with the observed low frequency Raman spectra (Takashige and Nakamura 1980, Srinivasan *et al* 1983). Unfortunately, the experimental data in this range of the phonon spectrum are far from the required resolution for a reliable frequency assignment. Up to now, neutron scattering measurements have been mainly devoted to study of the incommensurate characteristics of $[\text{N}(\text{CH}_3)_4]_2\text{ZnCl}_4$, leaving aside a careful determination of the dispersion curves. Therefore a precise rigorous construction of the specific heat curve should be abandoned. However, these low frequency modes are mostly responsible for the specific heat behaviour in the very low temperature range as their contribution to the specific heat rapidly saturates at relatively low temperatures. For this reason, the specific heat between 60 and 330 K is not greatly affected by a rough approximation of the low frequency phonon spectrum. Therefore, the most relevant Raman bands found in this region at 63 cm^{-1} and 70 cm^{-1} have been used in our estimation of the external mode contributions to the specific heat in $[\text{N}(\text{CH}_3)_4]_2\text{ZnCl}_4$.

Two points should be finally noted. (i) Due to the relative lack of sensitivity of the specific heat to notable changes in the phonon spectrum, small shifts in the estimated frequencies would only alter the specific heat within the margins of the experimental error (0.1%). (ii) Raman and/or infrared data at low temperatures could be of great interest as some inactive modes in the orthorhombic phase are active in the lower symmetry phases present at low temperatures. Unfortunately, the provisional frequency assignment to the inactive modes by the procedures described above shows that they probably overlap the peaks of the active mode frequencies.

Table 1. Normal modes in $[\text{N}(\text{CH}_3)_4]_2\text{ZnCl}_4$. The symmetries, the associated frequencies and their respective degeneracies are also indicated (Srinivasan *et al* 1983, Tang *et al* 1986, Meekees 1987, Meekees *et al* 1988, Gómez-Cuevas *et al* 1981). The assigned frequencies for T_1 and A_2 inactive modes were suggested by the methods described in the text.

Assignment	Activity	Symmetry	Degeneracy	Frequency (cm^{-1})
External	Raman		18	63–70
$\delta_{\text{Zn-Cl}}$	Raman	E	2	132
	Raman + IR	T_2	3	132
$\nu_{\text{Zn-Cl}}$	Raman + IR	A_1	1	277
	Raman + IR	T_2	3	277
$\delta_{\text{C-N}}$	Raman	E	2	374
	Raman + IR	T_2	3	460
$\nu_{\text{C-N}}$	Raman	A_1	1	757
	Raman + IR	T_2	3	954
$\delta_{\text{C-H}}$	Raman	A_1	1	280
	Raman	E	2	1174
	Raman	E	2	1457
	Raman + IR	T_2	3	1068
	Raman + IR	T_2	3	1284
	Raman + IR	T_2	3	1420
	—	T_1	3	1424
	—	T_1	3	909
	—	T_1	3	260
	—	A_2	1	260
	$\nu_{\text{C-H}}$	Raman	A_1	1
Raman		E	2	3028
Raman + IR		T_2	3	3028
Raman + IR		T_2	3	2950
—		T_1	3	3000

4. Lattice specific heat

Table 1 shows the schematic frequency spectrum used to obtain the $[\text{N}(\text{CH}_3)_4]_2\text{ZnCl}_4$ specific heat. It also accounts for the weights assigned to each frequency in agreement with the degeneracy of each mode. The lowest frequency (63 cm^{-1}) has been treated by a Debye function and the remaining ones by fixed frequency Einstein functions.

In figure 2, the specific heat obtained by this procedure and the experimental values are compared. The contribution of the internal modes of both tetrahedra and the external vibrations are also plotted in the same figure. At room temperature, a noticeable specific heat saturation of the external modes (98%) and the internal modes of the inorganic group (92%) should be noted. This is the result one should expect from the low frequencies of the corresponding modes (below 300 cm^{-1}) and from the Rb_2ZnCl_4 specific heat, which also approaches the saturation value (94%) at room temperature. On the other hand, lower specific heat values far enough from the saturation value (51%) are attained by the tetramethylammonium internal motions, because of the high C–N bond strength.

This effect is reinforced in the case of the methyl bending contribution (26%). However, a close saturation value (90%) is attained from the pure undeformed rotation

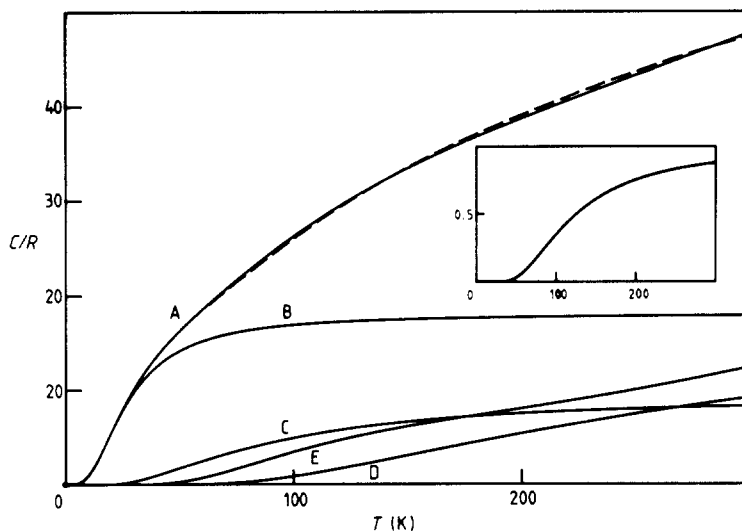


Figure 2. The various contributions to the lattice specific heat of $[\text{N}(\text{CH}_3)_4]_2\text{ZnCl}_4$. The broken curve represents the specific heat at constant volume. Curve A shows the harmonic specific heat obtained from the vibrational spectrum. The remaining full curves represent contributions that arise from: (B) the external modes of the inorganic and the two organic tetrahedra; (C) the inorganic group internal motions; (D) the C–N bending and stretching modes; (E) the methyl groups. The inset shows the specific heat associated with each undeformed rotation of the methyl groups.

of these groups around the three-fold C–N axis. This noticeable contribution to the specific heat is a new confirmation of the methyl highly activated rotational motions at room temperature which was previously deduced from C_p measurements (Ruiz-Larrea *et al* 1981) and independently established by other experimental techniques (Blinic *et al* 1979, Sundaram *et al* 1986, Arumugam *et al* 1987). The methyl rotation specific heat is shown in the inset of figure 2. It also agrees with the observed freezing of these modes below 60 K (Arumugam *et al* 1987).

A macroscopic approach can also be used in order to analyse the different contributions to the $[\text{N}(\text{CH}_3)_4]_2\text{MCl}_4$ specific heat. For this purpose, the specific heat of related crystals can be used for a comparative study. The tetramethylammonium contribution can be calculated from the specific heats of $[\text{N}(\text{CH}_3)_4]_2\text{FeCl}_4$ (Ruiz-Larrea *et al* 1988) and $\text{N}(\text{CH}_3)_4\text{FeCl}_4$ (Ruiz-Larrea *et al* 1987) as the two molecules only differ in one tetramethylammonium group. Under the assumption of unaffected internal frequencies, we can expect the subtraction of both specific heat curves to give a rough approximation of the $[\text{N}(\text{CH}_3)_4]$ contribution between 50 and 330 K—as in this range a nearly constant specific heat related to the external modes can be considered. In figure 3, we show these results with no anharmonic corrections and excluding the phase transition anomalies. The fit to the $[\text{N}(\text{CH}_3)_4]$ spectroscopic specific heat obtained above has been empirically adjusted by the Nernst–Lindemann law and is also plotted in the same figure. The value for the Nernst–Lindemann constant: $a = 1.2 \times 10^{-5} \text{ R}^{-1} \text{ K}^{-1}$, differs considerably from the one found for the complete $[\text{N}(\text{CH}_3)_4]_2\text{ZnCl}_4$ molecule. This result arises from the different elastic and expansivity properties of the iron substituted tetramethylammonium crystals (unknown) as well as from the intrinsic properties of the $[\text{N}(\text{CH}_3)_4]$ group.

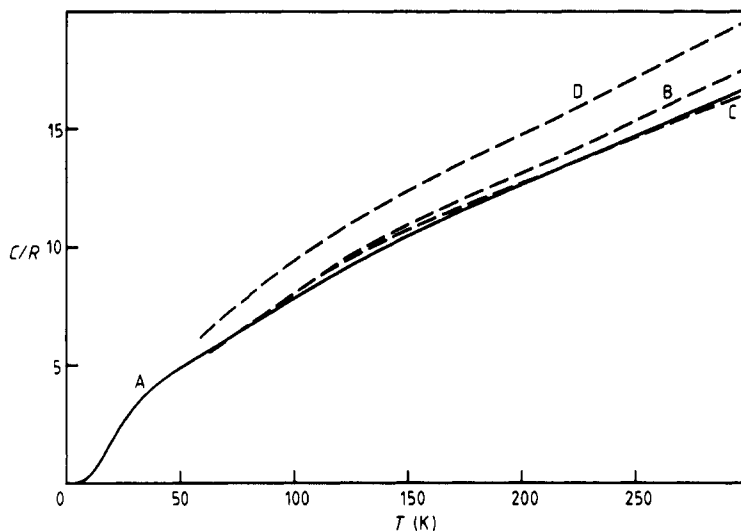


Figure 3. Tetramethylammonium contribution to the specific heat in $[\text{N}(\text{CH}_3)_4]_2\text{ZnCl}_4$. Curve A has been calculated from the corresponding frequencies of the spectrum (see table 1). Curve B represents the difference between the $[\text{N}(\text{CH}_3)_4]\text{FeCl}_4$ and $[\text{N}(\text{CH}_3)_4]_2\text{FeCl}_4$ specific heats at constant pressure. Curve C is obtained from curve B by subtraction of an empirical Nernst–Lindemann correction (see text). As a reference, we also show (curve D) the specific heat at constant pressure of $(\text{CH}_3)_4\text{Cl}$ (Chang and Westrum 1962). The phase transition anomalies have been omitted.

Direct subtraction of the specific heats of $[\text{N}(\text{CH}_3)_4]_2\text{ZnCl}_4$ and $[\text{N}(\text{CH}_3)_4]\text{FeCl}_4$ also leads to a good fit with the calculated $[\text{N}(\text{CH}_3)_4]$ contribution. This fact is particularly interesting as we have not performed the required corrections for the cation substitution by a corresponding states law. Discrepancies below 100 K could again be explained by shifts in the low frequency spectrum.

As cited before, the copper compound shows an anomalous behaviour and should be treated separately. Not only is its inclusion in the common pressure–temperature phase diagram still ambiguous, but also its thermodynamic properties (Gómez-Cuevas *et al* 1983) show remarkable differences with the remaining chloride compounds. The specific heat of the copper crystals at room temperature—just above the normal–incommensurate phase transition—reaches a higher value ($\approx 56R$) than the one found in $[\text{N}(\text{CH}_3)_4]_2\text{ZnCl}_4$ ($\approx 52R$). At first sight, this result should be the consequence of some relevant shifts of the spectrum to the low frequency region, as it would increase the specific heat value. However, the bands associated with the organic groups are practically the same as the ones found in $[\text{N}(\text{CH}_3)_4]_2\text{ZnCl}_4$ or in $[\text{N}(\text{CH}_3)_4]\text{Cl}$. The Raman and infrared spectra below 300 cm^{-1} also show some interesting features: owing to the Jahn–Teller flattening of the inorganic tetrahedron from the T_d to D_{2d} point group, the CuCl_4 internal mode frequencies are expected to differ from the ones in the undeformed ZnCl_4 . From previous Raman and infrared data (Gómez-Cuevas 1981, Gómez-Cuevas *et al* 1983) we can assign the band at 280 cm^{-1} to the Cu–Cl symmetric stretching (A_1). Although this mode is IR inactive in the ideal tetrahedron, that band appears in the IR spectrum due to the splitting of the asymmetric stretching T_2 (T_d point group) in modes B_2 and E (D_{2d} point group), both of which are IR active. B_2 can be

assigned to the band at 280 cm^{-1} and E is observed to shift to 235 cm^{-1} . The five Cu–Cl bending modes E and T_2 (T_d) also split into A_1 , B_1 , B_2 and E (D_{2d}), with frequencies that lie between $110\text{--}130\text{ cm}^{-1}$. Again, a small shift from the bending mode frequencies in the ZnCl_4 tetrahedron should be noted. However, this significant change of the frequency spectrum can only account for an increase of only $0.2R$ with respect to the $[\text{N}(\text{CH}_3)_4]_2\text{ZnCl}_4$ specific heat value at room temperature, which is far from the experimental difference ($\approx 4R$). Of course, the tetrahedral distortion surely affects the frequency spectrum of the external modes, but negligible effects on the specific heat can arise due to the near saturated value induced by frequency modes below 100 cm^{-1} at room temperature. The behaviour of the $[\text{N}(\text{CH}_3)_4]_2\text{CuCl}_4$ heat capacity could probably only be explained by a high anharmonic correction above the normal–incommensurate phase transition. It should also be in agreement with the excellent fit to the $[\text{N}(\text{CH}_3)_4]_2\text{ZnCl}_4$ specific heat below 230 K , as the anharmonic effect becomes insignificant at low temperatures.

A similar analysis of the lattice contribution can be carried out on the bromide and the iodide derivatives of the tetramethylammonium salts. In these cases the inorganic group internal modes are progressively moved to low frequencies along the halogen sequence: Cl–Br–I. This is a consequence of the decreasing values for the force constants, which shift the metal–halogen stretching mode from approximately 280 cm^{-1} (Cl–M) to 210 cm^{-1} (Br–M) and to 170 cm^{-1} (I–M) (Sabatini and Sacconi 1964). Substitution of the metallic cation only causes small changes in this frequency assignment. Assuming unaffected $[\text{N}(\text{CH}_3)_4]$ internal motions, higher specific heat values are expected when Cl^- is substituted by Br^- or by I^- above the low temperature range affected by the external modes. This is just the effect observed in $[\text{N}(\text{CH}_3)_4]_2\text{CuBr}_4$, the only bromide compound for which adiabatic results have been obtained up to now (López-Echarri *et al* 1989). However, this is not a conclusive result since the anharmonic contribution is not known and the general behaviour of the copper crystal is also anomalous within the frame of the bromide family. The heat capacities as well as the elastic constants and the thermal expansion coefficients of bromide and iodide salts are required for a definite conclusion.

5. Conclusion

The frequency assignment of the normal modes in $[\text{N}(\text{CH}_3)_4]_2\text{ZnCl}_4$ has permitted a reasonable calculation of the harmonic specific heat. It has also been shown that modes between 100 cm^{-1} and 1500 cm^{-1} are mostly responsible for the specific heat behaviour in the $60\text{--}330\text{ K}$ temperature range. The specific heat contribution of the tetramethylammonium groups obtained by this procedure is also in agreement with the one calculated by simple subtraction of the $[\text{N}(\text{CH}_3)_4]_2\text{FeCl}_4$ and $[\text{N}(\text{CH}_3)_4]\text{FeCl}_4$ specific heats. This result is a consequence of the practical lack of sensibility of the tetrahedral internal frequencies to changes in the surrounding crystal lattice. Noticeable small discrepancies only appear in the low temperature range and are explained by the contribution of the low frequency external modes ($<100\text{ cm}^{-1}$) which are more dependent on the crystal structure. This comparative study reinforces the importance of accurate specific heat data as they supply information that is usually obtained by microscopic experimental techniques. On the other hand, the analysis of the various contributions to the specific heat describes quite well the thermal motion of the different molecular units. In particular, the near saturated value attained by the methyl groups at

room temperature confirms the rapid undeformed rotation around the C–N three-fold axes.

We should also point out the excellent fit of the harmonic specific heat to the baseline previously obtained by extrapolation of the Debye temperature at both sides of the second-order phase transition—once a convenient anharmonic correction is performed. For this reason, only small errors are expected in the values of the phase transition thermodynamic functions, when this simple baseline is adopted.

Two main sources of errors in the analysis performed above will be finally cited.

(i) The Nernst–Lindemann law is used to estimate the elastic and thermal expansivity data throughout the whole temperature range. However, the anomalies which these magnitudes are expected to undergo when phase transitions are present would also make the anharmonic correction in the corresponding temperature region unreliable, even if such experimental information were available.

(ii) The influence of temperature in the phonon spectrum has also been discarded. This can be accomplished from a detailed knowledge of the temperature dependence of the various frequencies (Miller and Brockhouse 1971). However, this correction is expected to be negligible as the Raman and IR spectra of $[\text{N}(\text{CH}_3)_4]_2\text{ZnCl}_4$ do not show relevant changes from 77 to 300 K.

The calculated specific heat fits the experimental curve within 1% between 60 K and 330 K. A better approximation—up to the estimated 0.1% experimental error—could only be attained through a more accurate description of the phonon spectrum by means of inelastic neutron scattering. The resolution of the low frequency range ($<100\text{ cm}^{-1}$) would also account for the small specific heat differences found in the remaining isomorphous compounds.

Acknowledgments

This work was supported by CAYCIT (Spain) and by UPV/EHU (Universidad del País Vasco, Spain). We are indebted to A Criado (Universidad de Sevilla, Spain) and to C Santiago (UPV/ETH) for valuable information on the normal modes in organic molecules. We also thank Dr E H Bocanegra (UPV/EHU) for his kind help in the preliminary DSC measurements of the various tetramethylammonium compounds.

References

- Arumugam S, Murthy K, Srinivasan R and Bhat V S 1987 *Phase Trans.* **9** 259
- Berger J and Benoit J P 1984 *Solid State Commun.* **49** 541
- Blinic R, Burgar M, Slak J, Rutar V and Milia F 1979 *Phys. Status Solidi a* **56** K65
- Brun T O, Curtiss L A, Iton L E and Kleb R 1987 *J. Am. Chem. Soc.* **109** 4118
- Chang S S and Westrum E F 1962 *J. Chem. Phys.* **36** 2420
- Echegut P, Gervais F and Massa N E 1984 *Phys. Rev. B* **30** 6039
- Gesi K 1986 *Ferroelectrics* **66** 269
- Gómez-Cuevas A 1981 *PhD Thesis* Universidad del País Vasco, Spain
- Gómez-Cuevas A, López-Echarri A, Tello M J and Vidaurrázaga P 1981 *Ferroelectrics* **36** 339
- Gómez-Cuevas A, Tello M J, Fernández J, López-Echarri A, Herreros J and Couzi M 1983 *J. Phys. C: Solid State Phys.* **16** 473
- Gopal E S R 1966 *Specific Heats at Low Temperatures* (London: Heywood Books)
- Hasebe K, Mashiyama H and Tanisaki S 1982 *J. Phys. Soc. Japan* **51** 2049

- López-Echarri A, Ruiz-Larrea I and Tello M J 1989 *Phys. Status Solidi b* **154** 143
- Meekes H 1987 *PhD Thesis* Nijmegen University
- Meekes H, Janner A and Janssen T 1988 *Z. Phys. B* **71** 273
- Miller A P and Brockhouse B N 1971 *Can. J. Phys.* **49** 704
- Petzelt J, Volkov A A, Kozlov G V, Lebedev S P and Chapelle J P 1982 *J. Physique* **43** 1359
- Ruiz-Larrea I, López-Echarri A and Tello M J 1981 *J. Phys. C: Solid State Phys.* **14** 3171
- 1987 *Solid State Commun.* **64** 1099
- 1988 *Ferroelectrics* **73** 3116
- Sabatini A and Sacconi L 1964 *J. Am. Chem. Soc.* **86** 17
- Sawada S, Shiroishi Y, Yamamoto A, Takashige M and Matsuo M 1978a *Phys. Lett.* **67A** 56
- 1978b *J. Phys. Soc. Japan* **44** 687
- Sawada S, Yamaguchi S T, Suzuki H and Shimizu H 1985 *J. Phys. Soc. Japan* **54** 3129
- Shimizu H, Kokubo N, Yasuda N and Fujimoto S 1980 *J. Phys. Soc. Japan* **49** 223
- Shimizu H, Oguri A, Abe N, Yasuda N, Fujimoto S, Sawada S, Shiroishi Y and Takashige M 1979 *Solid State Commun.* **29** 125
- Srinivasan V, Subramanian C K and Narayanan P S 1983 *Indian J. Pure Appl. Phys.* **21** 271
- Sundaram C S, Ramakrishna J, Chandrasekhar K and Sastry V S S 1986 *Ferroelectrics* **69** 299
- Takashige M and Nakamura T 1980 *Ferroelectrics* **24** 143
- Tang S H, Looi E C and Radhakrishna S 1986 *Phys. Status Solidi b* **135** 519
- Tanisaki S and Mashiyama H 1980 *J. Phys. Soc. Japan* **48** 339
- Warshel A and Lifson S 1970 *J. Chem. Phys.* **53** 582
- Wiesner J R, Srivastava R C, Kennard C H L, Di Vaira M and Lingafelter E C 1967 *Acta Crystallogr.* **23** 565
- Zangar H, Miane J L and Daoud A 1983 *J. Phys. C: Solid State Phys.* **16** 6875
- Zubillaga J, López-Echarri A and Tello M J 1988 *J. Phys. C: Solid State Phys.* **21** 4417